

SENSOR AND SIMULATION NOTES

Note 234

CLEARED
FOR PUBLIC RELEASE

PL/PA 31.030 96

September 1977

COUPLING OF ELECTROMAGNETIC FIELDS FROM
AN ELECTRIC DIPOLE SOURCE TO A CONDUCTING SPHERE

by

Frederick M. Tesche

Science Applications, Inc.
Berkeley, California 94701

ABSTRACT

This note illustrates how electromagnetic energy is coupled from an electric dipole source to a perfectly conducting spherical body. The basic motivation for this work is to develop a method for simulating the effects of system-generated EMP (SGEMP) on large, complicated satellite systems. One recent concept for such a simulation is to experimentally measure the system response using a point source in the vicinity of the system. In this study, only an electric dipole source is considered and the satellite is represented by a sphere. The SEM coupling coefficients are then calculated for some of the lower natural resonances of the sphere, for various source locations and orientations.

PL 96-1077

SENSOR AND SIMULATION NOTES

Note 234

September 1977

COUPLING OF ELECTROMAGNETIC FIELDS FROM
AN ELECTRIC DIPOLE SOURCE TO A CONDUCTING SPHERE

by

Frederick M. Tesche
Science Applications, Inc.
Berkeley, California 94701

ABSTRACT

This note illustrates how electromagnetic energy is coupled from an electric dipole source to a perfectly conducting spherical body. The basic motivation for this work is to develop a method for simulating the effects of system-generated EMP (SGEMP) on large, complicated satellite systems. One recent concept for such a simulation is to experimentally measure the system response using a point source in the vicinity of the system. In this study, only an electric dipole source is considered and the satellite is represented by a sphere. The SEM coupling coefficients are then calculated for some of the lower natural resonances of the sphere, for various source locations and orientations.



I. Introduction

In attempting to simulate the SGEMP effects on spacecraft, a novel technique has been recently suggested by Baum⁽¹⁾. The basic simulation scheme involves measuring a transfer function between an infinitesimal current element outside the system under test and a critical circuit element buried within the system. Using a calculated SGEMP response for the volume currents surrounding the system, the measured system response can be treated as a Green's function, such that a weighted integral over the volume currents in the region surrounding the system yields the total SGEMP response at the circuit level. This simulator concept, referred to as DIES, is discussed in Ref. (2).

This approach is particularly useful in view of the present inability to model accurately the electrical behavior of the interiors of large, complicated systems. The exterior problem, on the other hand, is much more amenable to analysis using present-day SGEMP codes.

To design such a hybrid experimental program, a number of theoretical questions must be considered. In the actual SGEMP problem, volume currents may surround the satellite for some distance as well as occur within the satellite. The simulation process, however, may permit only a limited number of source locations, thereby introducing errors in

the simulation. One important problem is to determine how far away from the test object must the transfer function measurements be made.

Clearly, if no SGEMP-produced currents flow within a particular region of space, it is not necessary to measure the system response due to a dipole source at that position. Similarly, if it can be shown that the coupling of energy from a source in the volume of space under consideration to the system is very weak, no measurements need be taken.

As an example of this latter point, a study of the coupling of energy from an infinitesimal current element to the exterior of the satellite would be worthwhile. Instead of computing the transient responses for surface currents at various observation points as a function of source location using a standard integral equation approach as in Jones⁽³⁾ and numerical Fourier transformation, the coupling coefficients used in the singularity expansion method (SEM)^(4,5) can be examined. Their behavior, as a function of distance between the satellite and dipole, leads to a decision regarding the limits of the experimental transfer function measurement.

The SEM concept as originally put forth by Baum⁽⁴⁾ describes the coupling of electromagnetic energy from a

source to a scattering body in terms of poles of the response function (such as the induced surface current on the body) which occur in the complex frequency plane associated with the Laplace transform of the transient response.

Associated with each pole is a natural mode and a coupling vector which are independent of the type of excitation. The coupling vector and the incident field define a coupling coefficient which does depend on such factors as angle of incidence and polarization of the incident field. With the pole locations, the natural modes and the coupling coefficients, the delta function time response of the scatterer may be rapidly computed. More general waveforms may then be treated by convolution techniques.

In addition to being able to easily compute the time domain response of a scatterer, this method provides a means to characterize the complete electromagnetic behavior of the obstacle by a few numbers. Once the natural frequencies, modes and coupling coefficients are known, a wide variety of scattering problems can be rapidly determined without having to re-solve the boundary value problem. From this standpoint, the singularity expansion method is clearly more desirable than the conventional frequency domain or direct time domain solutions.

In this study, we concentrate on the behavior of the SEM coupling coefficients for a current element in the

presence of a conducting sphere. Although the sphere may not be an ideal electrical model for an actual satellite, it will serve to illustrate the coupling coefficient behavior for a body of finite extent and will point the way for similar calculations involving a more realistic geometry.

II. SEM Background

The SEM representation for the surface current on a scattering body can be written as^(4,5,6,7)

$$\bar{J}(\bar{r}, s) = \sum_{\alpha} \eta_{\alpha}(s) \frac{\bar{v}_{\alpha}(\bar{r})}{s - s_{\alpha}} + \bar{W}_e(\bar{r}, s) \quad (1)$$

Pole pairs

where the following definitions are used:

- \bar{J} - vector surface current on scatterer
- \bar{r} - vector from origin to observation point on surface
- $s = (\Omega + i\omega)$ - complex frequency in Laplace domain
- s_{α} - complex natural resonances of the scatterer, occurring in complex conjugate pairs
- $\bar{v}_{\alpha}(\bar{r})$ - the natural current distribution or mode which exists at frequency s_{α}
- $\eta_{\alpha}(s)$ - coupling coefficient for α^{th} mode
- $\bar{W}_e(\bar{r}, s)$ - possible entire function of s existing in expansion

In this expression, the current modes, \bar{v}_α , and the natural frequencies, s_α , are independent of the excitation of the problem. Only the coupling coefficient, η_α , will depend upon the details of the incident field which excites the surface currents.

The transient response of the scatterer surface currents can be obtained by taking the inverse Laplace transform of Eq. (1). Noting that terms involving $1/(s-s_\alpha)$ transform into $e^{s_\alpha t}$ in the time domain, it is possible to write the time domain counterpart of Eq. (1) as:

$$\bar{J}(\bar{r}, t) = \sum_{\alpha} \eta_\alpha(s_\alpha) \bar{v}_\alpha(\bar{r}) e^{s_\alpha t} U(t-t_0)$$

Pole pairs

+ contribution at poles of $\eta_\alpha(s)$ (2)

+ contribution from entire function .

Here $U(t-t_0)$ is a unit step function which turns on at an appropriate time t_0 . If the delta function (in time) response is desired, the coupling coefficient $\eta_\alpha(s)$ has no poles and, as a result, the second term in Eq. (2) vanishes leaving only a temporal contribution from the entire function.

As may be noted from Eq. (2), each pole pair contributes an exponentially damped sinusoidal term to the overall

body current response. Previous investigations have shown that for highly resonant structures, such as a thin wire, only a few pole terms are needed to accurately calculate the current response⁽⁵⁾. For fatter, less resonant structures, such as a spheroid, it has been observed that usually more pole terms are required for the same degree of convergence.

The coupling coefficient, $\eta_\alpha(s)$, can be computed using the formalism outlined in Ref. 7. As Baum discusses in that report, the surface current, \bar{J} , must be a solution of an integral equation of the form

$$\int_S \bar{K}(\bar{r}, \bar{r}'; s) \cdot \bar{J}(\bar{r}', s) dS = \bar{F}(\bar{r}, s) \quad (3)$$

where \bar{K} is a dyadic kernel operator and relates the response to a delta function excitation. The domain of integration S is over the surface of the scattering body. The term $\bar{F}(\bar{r}, s)$ is the forcing function related to the incident electromagnetic field.

If the integral equation is formulated using a magnetic field approach, the forcing term is then proportional to the incident tangential magnetic field on the scatterer surface. On the other hand, an electric field formulation of the integral equation yields a different kernel \bar{K} and the forcing function \bar{F} is then related to the tangential incident electric field.

The natural modes of the scatterer are defined as those non-trivial solutions to the equation

$$\int_S \bar{K}(\bar{r}, \bar{r}'; s_\alpha) \cdot \bar{v}_\alpha(\bar{r}') dS' = 0 \quad . \quad (4)$$

Notice that this last equation also defines the natural frequencies s_α .

It is possible to define additional modes, $\bar{\mu}_\alpha(\bar{r})$, as the forward modes, or "coupling vectors", as

$$\int_S \bar{\mu}_\alpha(\bar{r}) \cdot \bar{K}(\bar{r}, \bar{r}'; s_\alpha) dS = 0 \quad . \quad (5)$$

With these definitions the coupling coefficient can be written as

$$\eta_\alpha(s) = \frac{\int_S \bar{\mu}_\alpha(\bar{r}) \cdot \bar{F}(\bar{r}, s) dS}{\int_S \int_S \bar{\mu}_\alpha(\bar{r}) \cdot \frac{d}{ds} K(\bar{r}, \bar{r}'; s) \Big|_{s=s_\alpha} \cdot \bar{v}_\alpha(\bar{r}') dS dS'} \quad (6)$$

As noted by Marin⁽⁶⁾, if the magnetic field integral equation is used in Eq. (3), the modes $\bar{\mu}_\alpha$ and \bar{v}_α are different. However, for symmetric kernels as encountered in the electric field integral equation, these two modes are

identical. Thus, using the E-field formulation, the coupling coefficient in Eq. (6) may be written as

$$\eta_{\alpha}(s) = \beta_{\alpha} \int_S \bar{v}_{\alpha}(r') \cdot \bar{E}^{inc}(\bar{r}, s) dS \quad (7)$$

where the incident electric field is shown explicitly and the denominator in Eq. (6) is represented simply by the scalar term β_{α} .

From this last equation, it is seen that the coupling coefficient is proportional to the integral of the dot product, the incident electric field, and the modal currents over the surface of the scatterer.

III. SEM Coupling Coefficients for a Perfectly Conducting Sphere

As an example of how a point dipole couples electromagnetic energy to a sphere, consider the configuration illustrated in Figure 1. A perfectly conducting sphere of radius a is located at the origin of the (x, y, z) coordinate system. An infinitesimal current element of moment $I d\ell$ is located at a distance given by z_D along the \hat{z} direction. A second rectangular coordinate system (x', y', z') is centered at the dipole position above the sphere. Relative to this primed coordinate system, the current element is inclined with angles θ_D and ϕ_D .

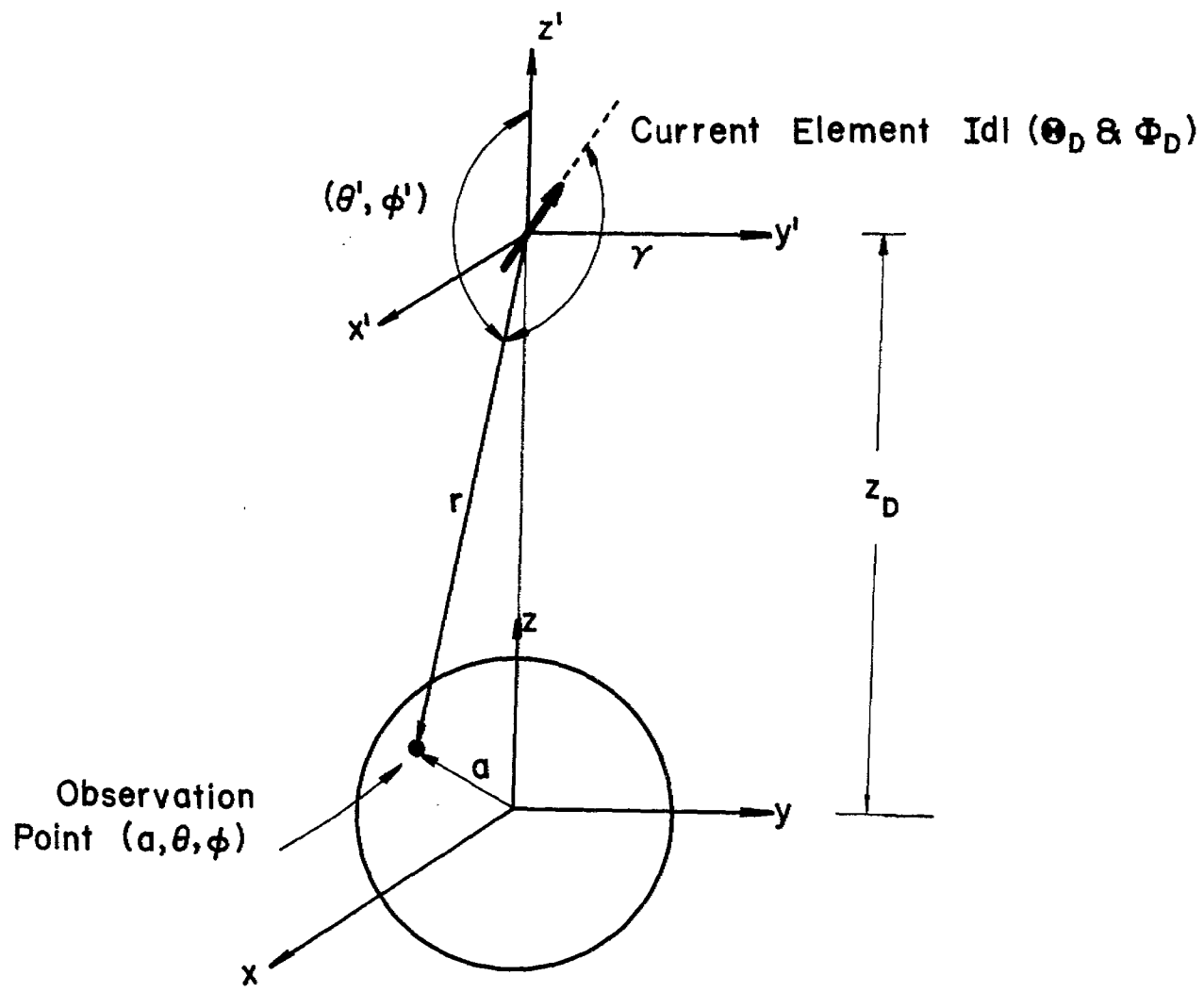


Figure 1. Geometry of the Problem

For this geometry and source configuration, we would like to calculate the coupling coefficients η_α at the various natural resonances s_α in order to study the coupling of energy from the dipole source to the satellite model. To accomplish this, the tangential electric field at the sphere from the dipole and the natural current modes are required for use in Eq. (7).

First, to evaluate the incident electric field, consider an observation point on the sphere surface, given by (a, θ, ϕ) . From the geometry of the problem, it can be easily shown that the distance, r , from the dipole to this observation point is given by

$$r = \sqrt{a^2 \sin^2 \theta + (z_D - a \cos \theta)^2} \quad . \quad (8)$$

In addition, the angles θ' and ϕ' can be defined as

$$\theta' = \arctan \left(\frac{a \sin \theta}{a \cos \theta - z_D} \right) \quad (9a)$$

and

$$\phi' = \phi \quad . \quad (9b)$$

The electric fields produced by an infinitesimal current element $Id\ell$ are discussed in Van Bladel⁽⁹⁾ and assume the following form in the complex frequency domain for

an observation point at a distance r from the source:

$$E_r = \frac{Z_0}{2\pi} \frac{Idl}{(sr/c)} e^{-sr/c} \left(\frac{s}{c}\right)^2 \cos\gamma \left[\frac{1}{sr/c} + \frac{1}{(sr/c)^2} \right] \quad (10)$$

and

$$E_\gamma = \frac{Z_0}{4\pi} \frac{Idl}{(sr/c)} e^{-sr/c} \left(\frac{s}{c}\right)^2 \sin\gamma \left[1 + \frac{1}{sr/c} + \frac{1}{(sr/c)^2} \right]. \quad (11)$$

In these equations Z_0 is the impedance of free space and c is the speed of light. The angle γ is between the direction of the dipole moment and the radius vector \bar{r} , as is indicated in Figure 1. Similarly, the electric field component E_γ is in the direction of the increasing γ angle.

Again, from elementary geometrical considerations, the angle γ between the dipole direction and observation point can be expressed as ⁽¹⁰⁾

$$\gamma = \arccos \left[\cos\theta_D \cos\theta' + \sin\theta_D \sin\theta' \cos(\phi - \phi_D) \right] \quad (12)$$

and the unit vector $\hat{\gamma}$ can be written as

$$\hat{\gamma} = \frac{1}{\sin\gamma} \left\{ \hat{\theta}' \left[\cos\theta_D \sin\theta' - \sin\theta_D \cos\theta' \cos(\phi' - \phi_D) \right] + \hat{\phi}' \left[\sin\theta_D \sin(\phi' - \phi_D) \right] \right\}. \quad (13)$$

With this last relation, it is possible to write the dipole field components in the primed coordinate system as:

$$E_r = \frac{Z_0}{2\pi} \frac{Id\ell}{(sr/c)} e^{-sr/c} \left(\frac{s}{c}\right)^2 \cos\gamma \left[\frac{1}{sr/c} + \frac{1}{(sr/c)^2} \right] \quad (14a)$$

$$E_{\theta'} = \frac{Z_0}{4\pi} \frac{Id\ell}{(sr/c)} e^{-sr/c} \left(\frac{s}{c}\right)^2 \left[\cos\theta_D \sin\theta' - \sin\theta_D \cos\theta' \cos(\phi - \phi_D) \right] \\ \times \left[1 + \frac{1}{(sr/c)} + \frac{1}{(sr/c)^2} \right] \quad (14b)$$

and

$$E_{\phi'} = \frac{Z_0}{4\pi} \frac{Id\ell}{(sr/c)} e^{-sr/c} \left(\frac{s}{c}\right)^2 \left[\sin\theta_D \sin(\phi' - \phi_D) \right] \\ \times \left[1 + \frac{1}{(sr/c)} + \frac{1}{(sr/c)^2} \right] \quad (14c)$$

To evaluate the coupling coefficients for the dipole near the sphere via Eq. (7), it is necessary to determine the tangential components of the dipole field on the sphere. These may be found by first converting E_r , $E_{\theta'}$, and $E_{\phi'}$ in Eqs. (14) to cartesian components at the sphere surface as

$$E_x = \sin\theta' \cos\phi' E_r - \sin\phi' E_{\phi'} + \cos\theta' \cos\phi' E_{\theta'} \quad (15a)$$

$$E_y = \sin\theta' \cos\phi' E_r + \cos\phi' E_{\phi'} + \cos\theta' \sin\phi' E_{\theta'} \quad (15b)$$

$$E_z = \cos\theta' E_r - \sin\theta' E_{\theta'} \quad (15c)$$

Then the electric field from the dipole may be re-expressed in spherical coordinates centered about the sphere as:

$$E_a = \sin\theta \cos\phi E_x + \sin\phi \sin\theta E_y + \cos\theta E_z \quad (16a)$$

$$E_\theta = \cos\theta \cos\phi E_x + \cos\theta \sin\phi E_y - \sin\theta E_z \quad (16b)$$

$$E_\phi = -\sin\phi E_x + \cos\phi E_y \quad (16c)$$

The latter two terms, (16b) and (16c), will be the components of the incident field used in evaluating Eq. (1).

In addition to the tangential incident electric field on the sphere, it is necessary to determine the natural modes for the sphere to determine the coupling coefficients.

The natural modes and natural frequencies of a sphere have been studied in detail in Refs. (4, 6 and 8). It is known that two types of natural modes exist. The first type of mode has the property that the surface divergence of the mode is zero, i.e., the mode has no surface charge associated with it. The second class of modes does have a non-zero divergence and corresponding surface charge. Baum⁽⁴⁾ distinguishes between these classes of modes through the use of an index q , with $q = 1$ referring to the modes with no surface charge density and with $q = 2$ for the other modes with a charge density.

The natural frequencies for the sphere, s_α , have been tabulated extensively in Ref. (8). The subscript α actually represents a number of different subscripts which serve to identify a particular natural mode or resonance. Specifically, α can be written as (q, n, n', m) where q is discussed above, n varies from 1 to infinity and is related to the order of the spherical Bessel function used in the wave function representation of the total surface current. The index n' indicates which root of the n^{th} spherical Bessel function is being considered, and the index m represents the order of the ϕ variation of the natural mode.

In Ref. (4), the natural current modes $\bar{v}_{q, n, n', m}(\theta, \phi)$ are shown to be

$$\bar{v}_{2, n, n', m}(\theta, \phi) = \frac{\partial P_n^m(\cos\theta)}{\partial\theta} e^{-im\phi} \hat{\theta} - \frac{P_n^m(\cos\theta)}{\sin\theta} im e^{-im\phi} \hat{\phi} \quad (17a)$$

for $q = 2$, and

$$\bar{v}_{1, n, n', m}(\theta, \phi) = -\frac{P_n^m(\cos\theta)}{\sin\theta} im e^{-im\phi} \hat{\theta} - \frac{\partial P_n^m(\cos\theta)}{\partial\theta} e^{-im\phi} \hat{\phi} \quad (17b)$$

for $q = 1$. In these equations, P_n^m is the associated Legendre polynomial. Notice that the index n' does not occur in the right-hand side of these equations.

With the previously derived electric field at the sphere surface given in Equation (16) and the expression for the natural current modes, the SEM coupling coefficients can then be written as an integral over the entire sphere surface as

$$\eta_{1,n,n',m} = \beta_{1,n,n',m} \int_0^\pi \int_0^{2\pi} \left(-im E_\theta(\theta, \phi) \frac{P_n^m(\cos\theta)}{\sin\theta} - E_\phi(\theta, \phi) \frac{\partial P_n^m(\cos\theta)}{\partial\theta} \right) e^{-im\phi} \times \sin\theta \, d\theta \, d\phi \quad (18a)$$

for the case $q = 1$ (no charge), and

$$\eta_{2,n,n',m} = \beta_{2,n,n',m} \int_0^\pi \int_0^{2\pi} \left(E_\theta(\theta, \phi) \frac{\partial P_n^m(\cos\theta)}{\partial\theta} - im E_\phi(\theta, \phi) \frac{P_n^m(\cos\theta)}{\sin\theta} \right) e^{-im\phi} \times \sin\theta \, d\theta \, d\phi \quad (18b)$$

for the case $q = 2$ (surface charge present). Note that in Equation (18), the coefficients, β_α , are still not defined.

They could be evaluated in terms of the double integral given in Equation (6) if exact numerical results are desired. In the present study, however, we shall investigate only relative variations of the various coupling coefficients, so that it will not be necessary to evaluate the β coefficients.

The natural frequencies for the sphere, $s_{q,n,n'}$, are illustrated in Figure 2. Only the upper left-hand portion of the complex plane is plotted, as there is complex conjugate symmetry about the $\Omega a/c$ axis. Notice that the index m does not occur in Figure 2, signifying that the natural resonances do not depend on this quantity. Only the natural modes (and therefore the coupling coefficients) will depend on the index m .

As has been noted in previous investigations, the singularities nearest the $j\omega$ axis are most important in determining the transient response for the surface currents. Moreover, for EMP excitation, the low frequency resonances usually have the largest excitation. Thus, in looking at the excitation of the sphere by the dipole, only the first few poles in Figure 2 will suffice. We will consider the behavior of the coupling coefficients for the first two resonances in both the first and second layer. These are the resonances with the values $q = 2, n = 1, n' = 1$ and $q = 1, n = 2, n' = 1$ for the second layer poles. The possible

values of the index m will depend on the spatial behavior of the incident field.

As a first example of the sphere excitation, the case of a radially directed dipole is considered. Since the dipole is located along the z axis above the sphere and has the orientation given by $\theta_D = 0$ and $\phi_D = 0$, only axially symmetric modes are excited. This implies that only for $m = 0$ will the integral in Eq. (7) have a non-vanishing result.

Figure 3 shows the behavior of the coupling coefficients for the first two resonances in the first layer closest to the $j\omega$ axis (the $q = 2$ layer). For convenience, the coupling coefficient is normalized by a reference coupling coefficient arising from an identical point dipole located at $z = 10a$. In addition, a multiplicative term $e^{sz_D/c}$ has been included in the dipole fields of Eq. (14) so as to locate the $t = 0$ reference point at the center of the sphere. In this manner, the exact value of the normalizing constant β_α in Equations (7) and (18), as well as the value of the current moment Idl , are not important. Due to the rapid growth of the magnitude of $(\eta_\alpha/\eta_{\alpha_{ref}})$ in the vicinity of the sphere, it is best to plot this quantity on a logarithmic scale.

Also plotted in this figure is the magnitude of $(z_{ref}/z_D)^2$ (the dotted lines). In inspecting Eqs. (10) and (11), the fields produced by the current element in the $\gamma = \pi$ direction are observed to fall off as $1/r^2$. Thus, for the dipole in the radial direction, it is to be expected that the coupling coefficient varies as $1/r^2$ for source

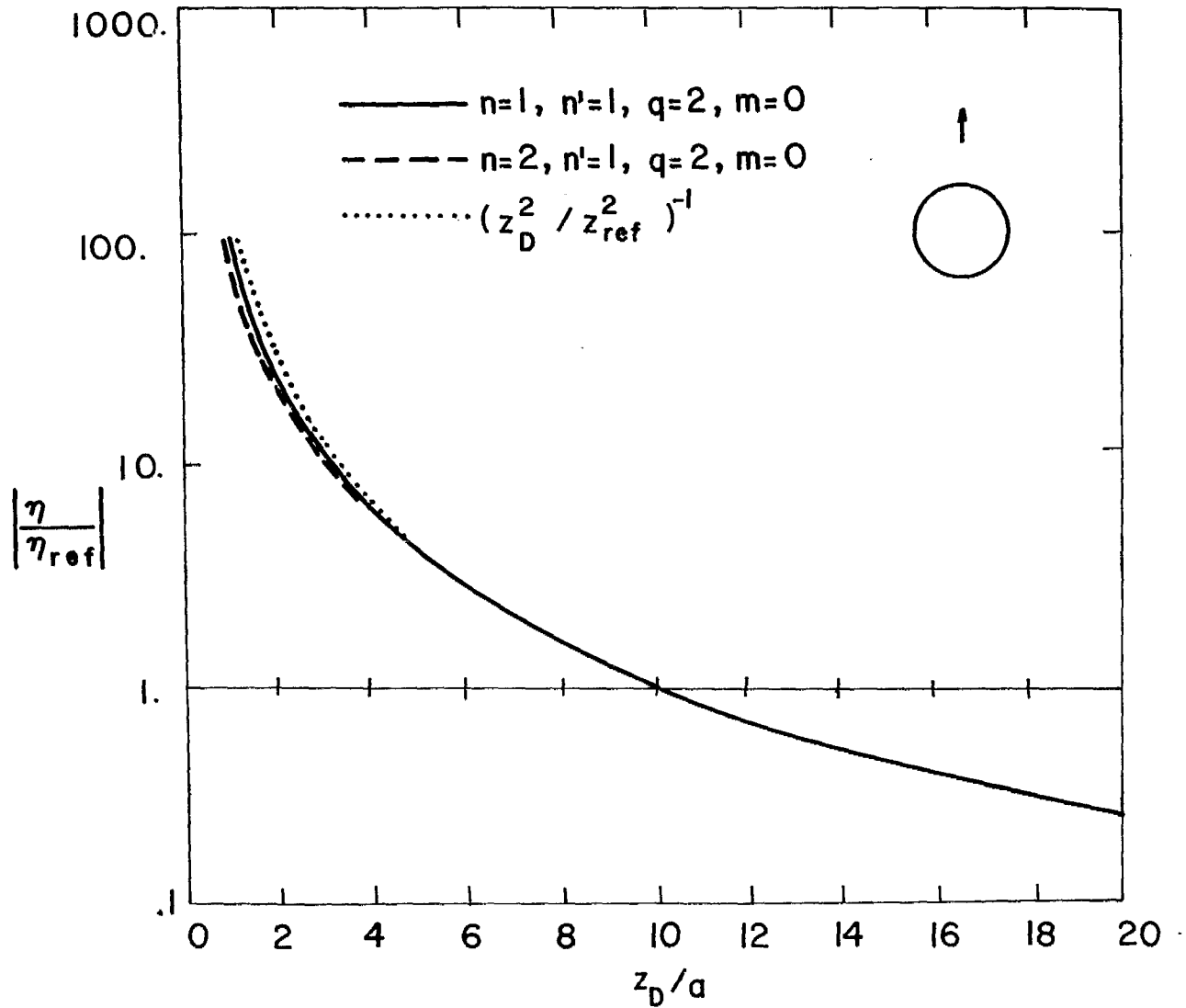


Figure 3. Relative Coupling Coefficient for Radial Current Element for $q=2$ Resonances

locations far from the sphere. For the first layer poles, it may be observed that for sources at a distance greater than about $4a$, the coupling is $1/r^2$ in nature. At closer distances, a $1/r^2$ variation of the coupling coefficient tends to slightly overestimate the coupling.

Figure 4 presents the same ratio of coupling coefficients for the resonances in the $q = 1$ layer. As before, only the $m = 0$ modes are excited due to the source orientation. Notice, however, that the $1/r^2$ curve tends to substantially overestimate the coupling of the fields.

The coupling coefficients for a current element in the $\theta_D = \pi/2$, $\phi_D = 0$ direction are presented in Figures 5 and 6 for the $q = 2$ and $q = 1$ layers respectively. For this type of excitation, the $m = 1$ modes are non-zero. Moreover, because the fields of the current element fall off as $1/r$ in the $\gamma = \pi/2$ direction, the coupling coefficients for this case can be expected to have a $1/r$ asymptotic behavior.

Figure 5 shows a very marked dip in the coupling coefficient in the vicinity of $z_D = 1.3a$. It is interesting to note that for the first resonance ($n = 1$, $n' = 1$) the coupling coefficient tends to increase less rapidly than $1/r$. The second coefficient for ($n = 2$, $n' = 1$), however, increases faster than $1/r$. The physical reason for these effects is not yet understood, and bears more thought.

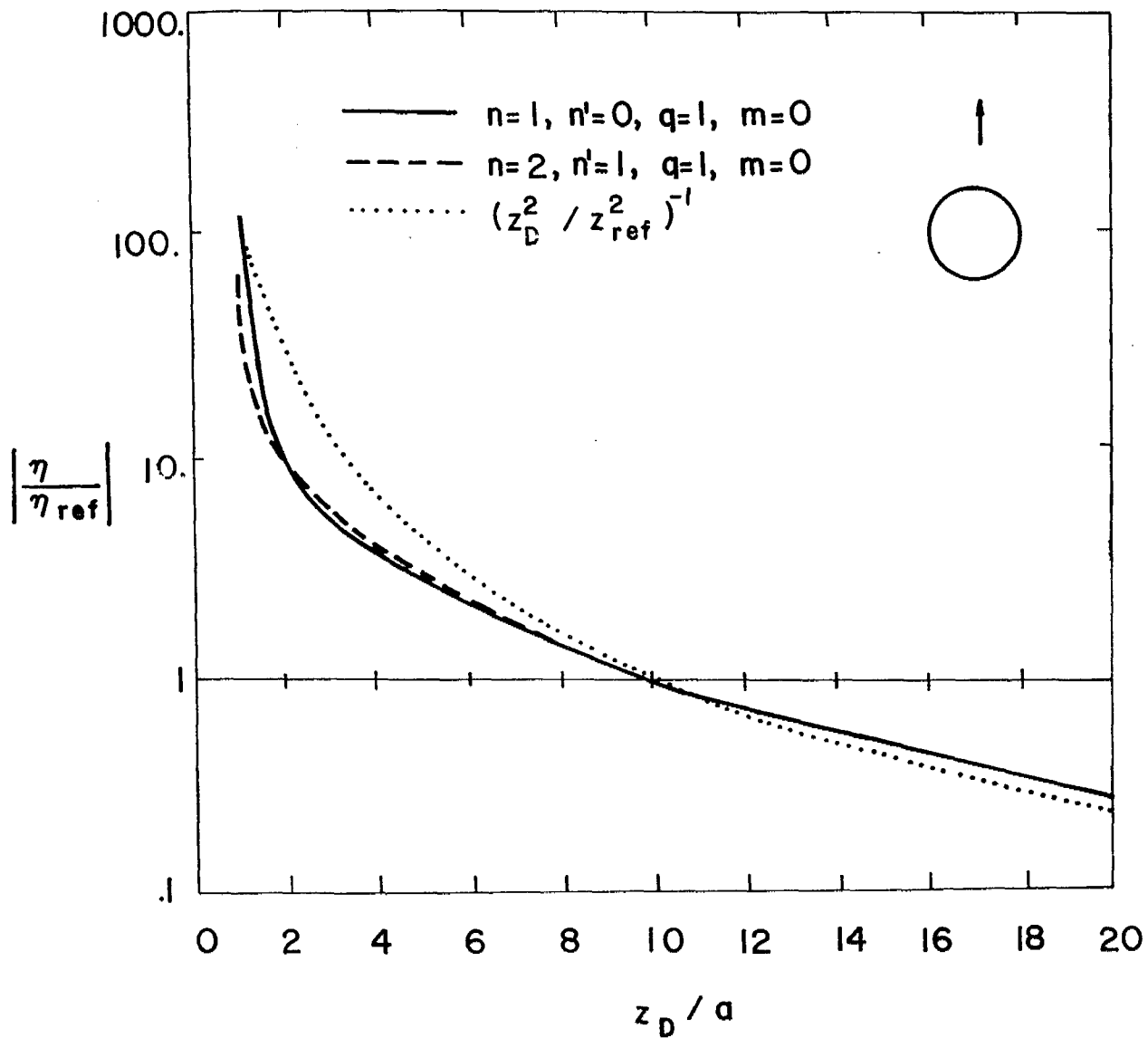


Figure 4. Relative Coupling Coefficient for Radial Current Element for $q = 1$ Resonances

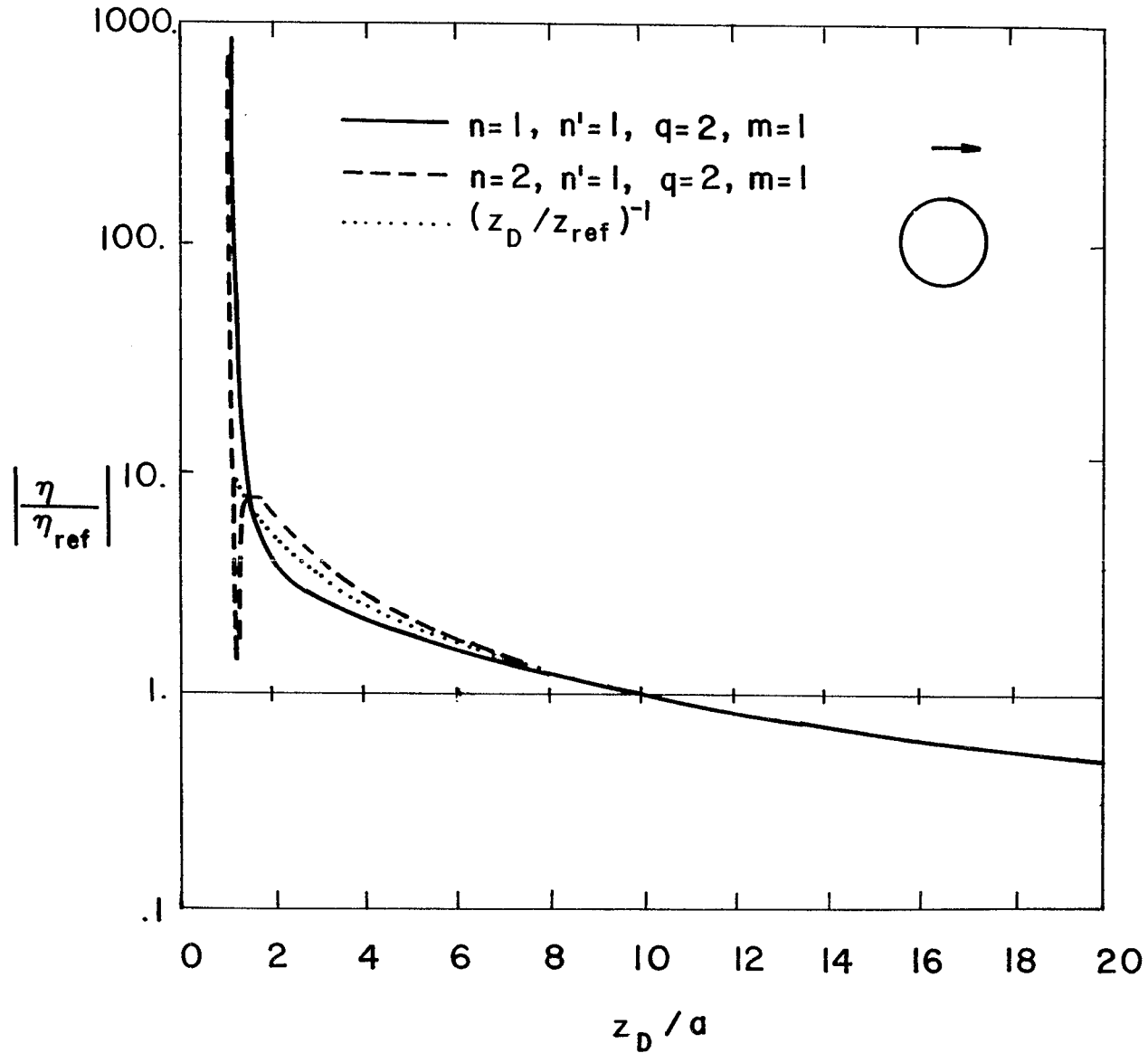


Figure 5. Relative Coupling Coefficient for Tangential Current Element for $q = 2$ Resonances

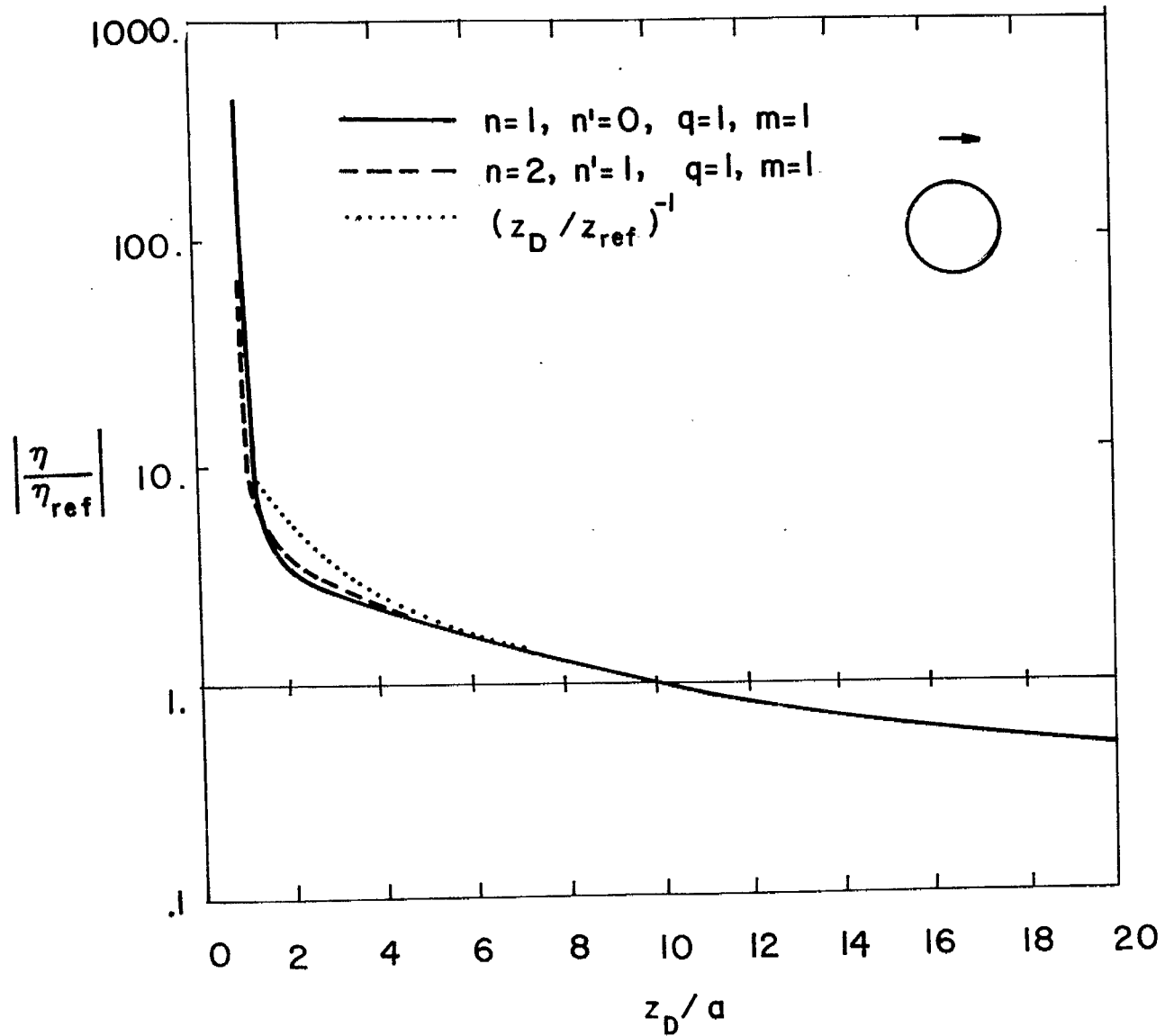


Figure 6. Relative Coupling Coefficients for Tangential Current Element for $q = 1$ Resonances

In the previous cases, the strength of the current element, $I dl$, remained constant as the source position was varied. If the current is allowed to increase in a manner which is proportional to the distance z_D , the field produced by the source in the broadside direction ($\gamma = \pi/2$) becomes planar in nature and approaches a constant in magnitude. In the limit as the source goes to infinity, the observed field is an incident plane wave.

In Ref. (8), the excitation of a sphere by a plane wave was considered in some detail. Moreover, actual (un-normalized) coupling coefficients were presented. In Figures 7 and 8, the coupling coefficient ratio $(\eta_\alpha / \eta_{\alpha_{pw}})$ is plotted as a function of the source position, z_D , for both the $q = 1$ and $q = 2$ modes. Here $\eta_{\alpha_{pw}}$ is the coupling coefficient for the incident plane wave and the set of parameters given by α .

As in the previous case where the dipole was in the tangential direction ($\hat{\theta}$ direction), only the $m = 1$ modes are excited. It is seen that by the time the source is at the position $z_D = 10a$, the coupling is almost identical to that produced by a plane wave.

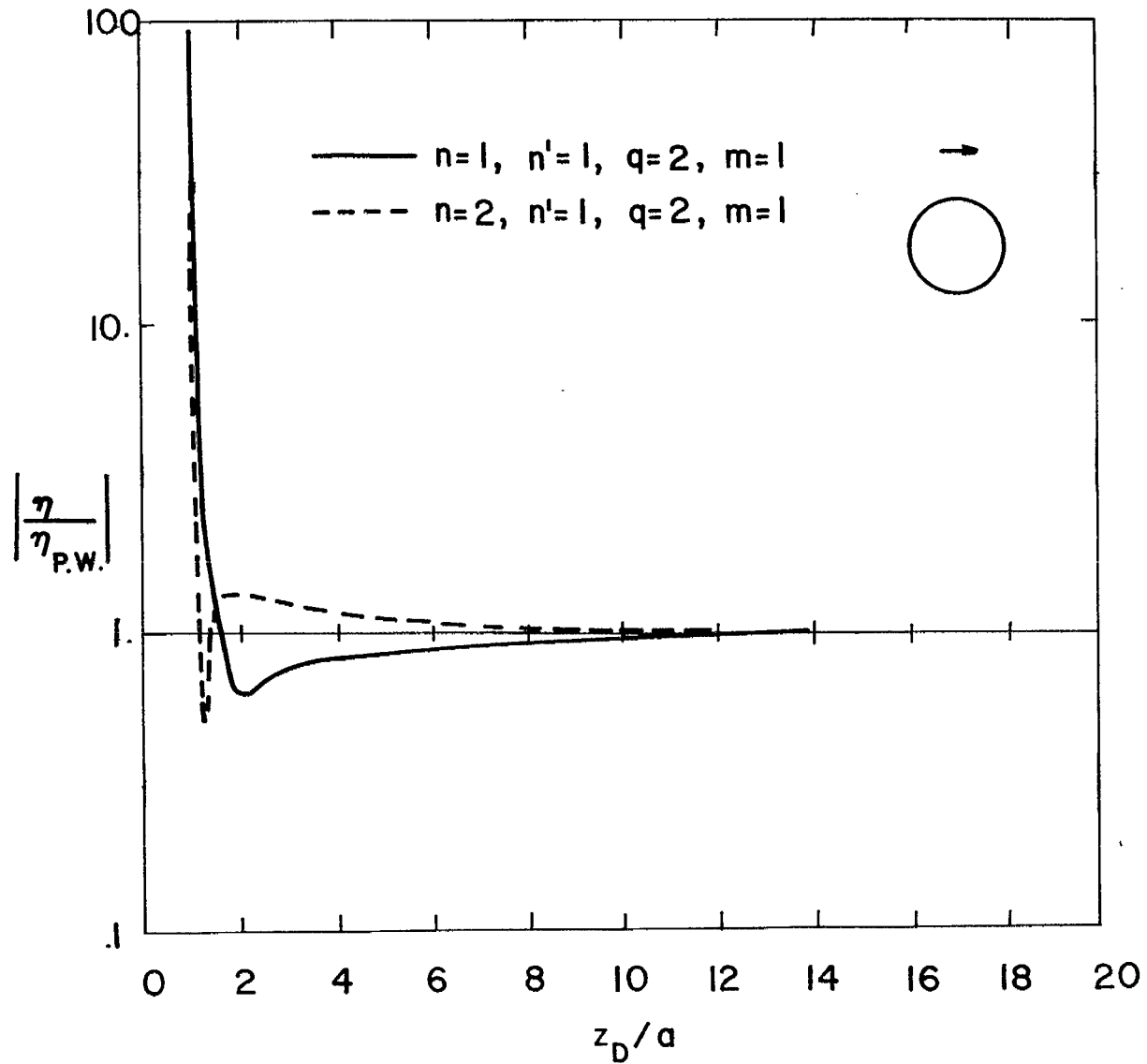


Figure 7. Coupling Coefficients Relative to Plane Wave Coefficients for $q = 2$ Resonances

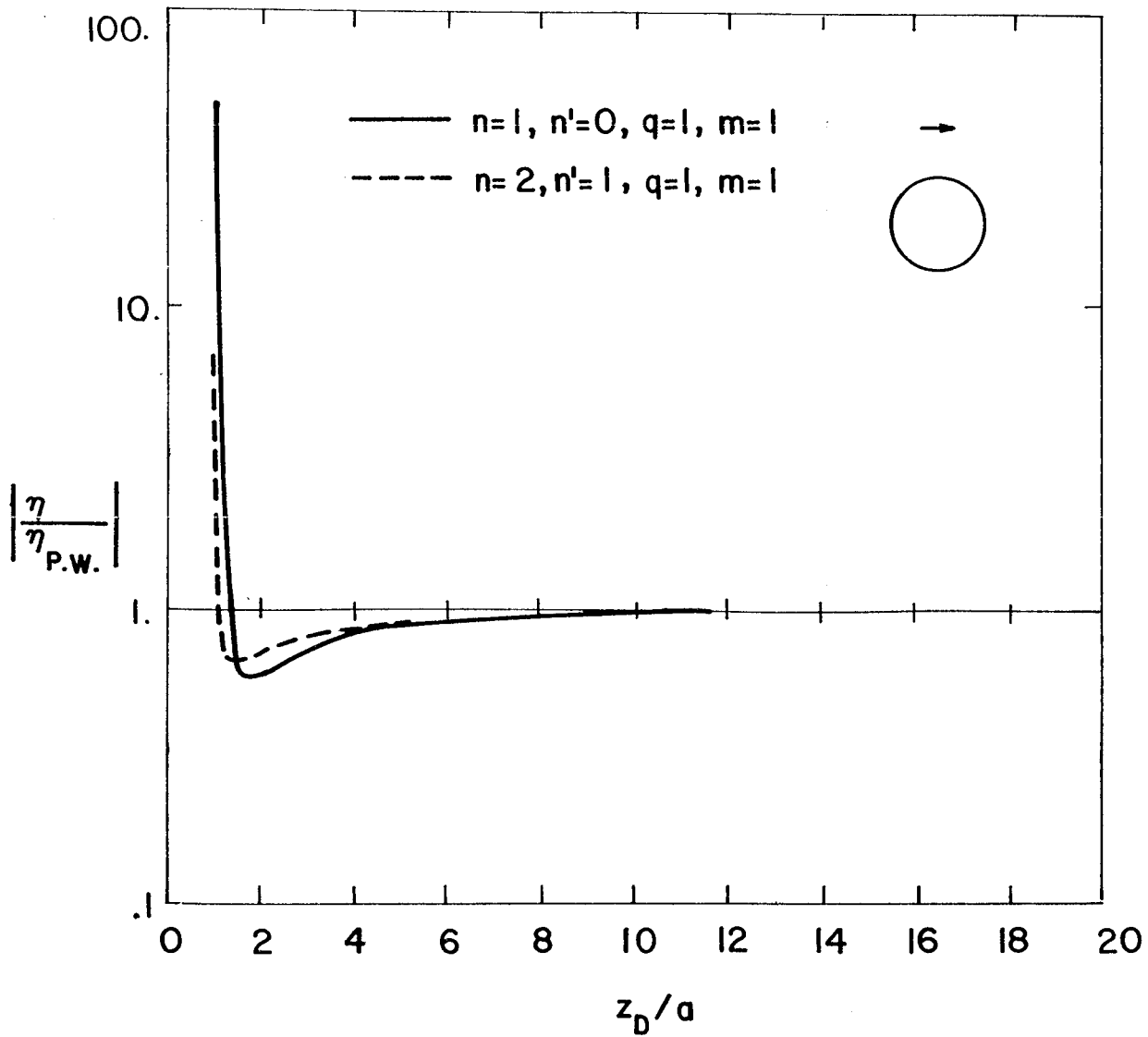


Figure 8. Coupling Coefficients Relative to Plane Wave Coefficients for $q = 1$ Resonances

IV. Conclusions

From the results presented here, a number of preliminary conclusions can be drawn regarding the possibility of simulating the SGEMP system response using this hybrid method. It is apparent that as source locations approach the surface of the sphere, the coupling of fields becomes very efficient. For most cases, the coupling tends to fall off by $1/r$ or $1/r^2$ (depending on the source orientation) once the source is outside a radius of roughly six times the sphere radius.

At this stage, it is not possible to define a precise limit on the size of the necessary source region surrounding the sphere, since this will depend on the magnitudes of the volume currents flowing about the sphere. For example, if there were an extremely large current source at $z_D = 12a$, it could provide most of the surface current excitation even though the coupling coefficient is a factor of 100 smaller than for a source near the sphere surface. Thus, the curves in Figures 5 through 8 must be used in conjunction with knowledge of the behavior of the calculated SGEMP volume currents.

Finally, from the studies of the coupling coefficients for the plane wave, it is seen that for tangential sources farther away than about $10a$, the coupling is very close to

that of an incident plane wave. This would suggest the possibility of using EMP simulator data to obtain the required transfer functions as well as making measurements for closer dipole sources.

REFERENCES

1. Baum, C.E., "EMP Simulators for Various Types of Nuclear EMP Environments: An Interim Categorization", adapted from AFWL SSN151, and submitted to the IEEE Trans. A.P. special issue on EMP.
2. Baum, C.E., "Some Types of Small EMP Simulators", Miscellaneous Simulator Memos, Memo 9, Dec. 22, 1976.
3. Jones, D.S., The Theory of Electromagnetism, Pergamon Press, 1964.
4. Baum, C.E., "On the Singularity Expansion Method for the Solution of Electromagnetic Interaction Problems", AFWL EMP Interaction Note 88, Dec. 11, 1971.
5. Tesche, F.M., "On the Singularity Expansion Method as Applied to Electromagnetic Scattering from Thin Wires", AFWL EMP Interaction Note 102, April 1972.
6. Marin, L., "Natural-Mode Representation of Transient Scattering from Rotationally Symmetric, Perfectly Conducting Bodies, and Numerical Results for a Prolate Spheroid", AFWL EMP Interaction Note 119, Sept. 1972.
7. Baum, C.E., "On the Singularity Expansion Method for the Case of First Order Poles", AFWL EMP Interaction Note 129, Oct. 24, 1972.
8. Martinez, J.P., Z.L. Pine, and F.M. Tesche, "Numerical Results of the Singularity Expansion Method as Applied to a Plane Wave Incident on a Perfectly Conducting Sphere", AFWL EMP Interaction Note 112, May 1972.
9. Van Bladel, J., Electromagnetic Fields, McGraw-Hill, 1964.
10. Du, L., and C.T. Tai, "Radiation Patterns for Symmetrically Located Sources on a Perfectly Conducting Sphere", Ohio State Research Foundation Report 169-10, Dec. 1964.